Published in final edited form as:

Eur J Inorg Chem. 2014 September ; 2015(25): 4109–4114. doi:10.1002/ejic.201402413.

Diiron Azamonothiolates via Scission of Dithiadiazacyclooctanes by Iron Carbonyls

Tai Lin[#], **Olbelina A. Ulloa**[#], **Thomas B. Rauchfuss**, and **Danielle L. Gray**

School of Chemical Sciences, University of Illinois, Urbana, IL 61801, United States

[#] These authors contributed equally to this work.

Abstract

The reaction of $Fe_3(CO)_{12}$ with the dithiadiazacyclooctanes $[SCH_2N(R)CH_2]_2$ affords $Fe_2[SCH_2N(Me)CH_2](CO)_6$ (R = Me, Bn). The methyl derivative **1**^{Me} was characterized crystallographically (Fe-Fe = 2.5702(5) Å). Its low symmetry is verified by variable temperature ^{13}C NMR spectroscopy which revealed that the turnstile rotation of the $S(CH_2)Fe(CO)_3$ and $S(NMe)Fe(CO)_3$ centers are subject to very different energy barriers. Although **1**^{Me} resists protonation, it readily undergoes substitution by tertiary phosphines, first at the $S(CH_2)Fe(CO)_3$ center, as verified crystallographically for $Fe_2[SCH_2N(Me)CH_2](CO)_5(PPh_3)$. Substitution by the chelating diphosphine dppe ($Ph_2PCH_2CH_2PPh_2$) gave $Fe_2[SCH_2N(Me)CH_2](CO)_4$(dppe), resulting from substitution at both the $S(CH_2)Fe(CO)_3$ and $S(NMe)Fe(CO)_3$ sites.

Introduction

The iron carbonyls form an immense range of complexes with organosulfur ligands. Curiously almost all such complexes result from degradation of organosulfur compounds. Only a fraction of organosulfur ligands bind intact to iron carbonyls.[1] This trend highlights the tendency of iron(0) compounds to break C-S bonds, which in turn highlights the apparent high stability of iron carbonyl thiolates.

Iron carbonyl derivatives of *S,N*-compounds were uncommon, at least they were prior to the proposed,[2] now confirmed,[3] occurrence of the azadithiolate cofactor in the [FeFe]-hydrogenases (Figure 1).

Although such diiron azadithiolates can be prepared by multiple routes,[4] such methods involve multistep conversions. We speculated that the $[(SCH_2)_2NR]^{2-}$ ligand (R-adt^{2-}) could arise from the degradation of 8- or 6-membered *S,N*-heterocycles by $Fe_3(CO)_{12}$. Sulfur-nitrogen heterocycles are attractive reagents because they can be made in high yields by condensation of primary amines with hydrogen sulfide and formaldehyde.[5] They are structurally related to the P_2N_2 ligands popularized by DuBois et al. (Figure 2) [6].

Correspondence to: Thomas B. Rauchfuss.

Supporting Information

Spectroscopic data on new compounds.

Our findings show that the $S_2N^R_2$ heterocycles are cleaved by $Fe_3(CO)_{12}$ to yield organoiron complexes with bridging -$CH_2N(R)CH_2S$- moieties.

Results and Discussion

Reactions of $S_2N_2R_2$ with Iron Carbonyls

The reaction of two equivalents of $Fe_3(CO)_{12}$ with $S_2N^R_2$ produced organoiron compounds with the formula $Fe_2[SCH_2N(R)CH_2](CO)_6$ (**1^R**, R = Me, Bn). The products were obtained in good yields as red colored powders after purification by column chromatography, which separates the product from $Fe(CO)_5$ and traces of $Fe_2(SCH_2S)(CO)_6$ (**2**). When the reaction was monitored by in-situ IR spectroscopy, we did not observe any intermediates. The synthesis can be represented by the idealized equation 1.

$$Fe_3(CO)_{12}+\tfrac{1}{2}[SCH_2\mathrm{N}(\mathrm{R})CH_2]_2 \rightarrow \underset{\substack{\mathbf{1^{Me}}\,(\mathrm{R}=Me)\\ \mathbf{1^{Bn}}\,(\mathrm{R}=Bn)}}{Fe_2[SCH_2\mathrm{N}(Me)CH_2](CO)_6}+Fe(CO)_5+CO \quad (1)$$

We propose that **2** arises via the reaction of $Fe_3(CO)_{12}$ with a small amount of S_2N^R generated by degradation of $S_2(N^R)_2$ during the synthesis of **1^{Me}**. Consistent with this scenario, we demonstrated that **2** forms in moderate yields from the reaction of $Fe_3(CO)_{12}$ with S_2N^{Me}. The infrared spectra of **1^{Me}** and **1^{Bn}** in the ν_{CO} largely resemble that of $Fe_2((SCH_2)_2NH)(CO)_6$, the bands for **1^R** being ~5 cm^{-1} lower in energy than those for $Fe_2((SCH_2)_2\,NH)(CO)_6$.

The structure of **1^{Me}** is supported by spectroscopic and crystallographic analysis. Two dimensional ^{1}H-^{1}H and ^{1}H-^{13}C correlation NMR spectra indicate that **1^{Me}** is chiral, and that the $Fe_2[SCH_2N(Me)CH_2]$ core is rigid. Signals for N*C*H_2S (δ4.62, 3.51, 2H; δ73.8, 1C) were assigned by comparison to the SCH_2S backbone of **2** (δ4.65, 2H); the FeCH_2N group was therefore assigned to be the more downshifted signals in both the ^{1}H and ^{13}C NMR spectra (δ 2.73, 3.02, 2H; δ57.8, 1C). To assign the two C-*H* centers associated with the 4-bond coupling ("W-coupling") in the spectrum of **1^{Me}**, we examined the dihedral angles of the -CH_2-N-CH_2-S-moiety containing the hydrogen atoms of interest (Table 1). Large W-coupling is associated with small dihedral angles (Φ).[7] Thus, since H_C and H_E are in planes with the smallest dihedral angle they will most likely exhibit the 4-bond coupling that is observed in the ^{1}H NMR spectrum (Table 1).

Crystallographic analysis confirmed that two $Fe(CO)_3$ centers are bridged by thiolate and iminium-like[8] ligands. The Fe centers differ in that one is bonded to nitrogen (Fe-N = 2.0332(17) Å), and the other to an alkyl ligand (Fe-CH_2 = 2.055(2) Å) (Figure 3). The Fe-Fe bond (2.5702(5) Å) is longer than related complexes with Fe_2S_2 cores (2.4924(7) Å).[4b] This elongation is attributed to the extended Fe-N(Me)-CH_2-Fe linkage. Long has described a related $Fe_2(CO)_6$ complex with a μ-pyridyl group.[9] The Fe-Fe distance in that complex is comparable to that in **1^{Me}**.

Cyclic voltammogram of **1^{Me}** at various scan rates show a quasi-reversible reduction at E_{pc} = -1.85 V vs $Fc^{0/+}$ in CH_2Cl_2 (see SI). In comparison, $Fe_2[(SCH_2)_2CH_2](CO)_6$ has been

reported in the range of E_{pc} = -1.61 to -1.74 V vs $Fc^{0/+}$ in MeCN, and $Fe_2[(SCH_2)_2CH_2](CO)_6$ is reduced at E_{pc} = -1.58 V vs $Fc^{0/+}$ in MeCN.[10] The shift in potential for **1**^{Me} in comparison to the iron dithiolate hexacarbonyl complexes may be partially attributed to the use of a less polar solvent. However, the more negative reduction potential for **1**^{Me} may also be attributed to increased electron density on the metal centers in comparison to the iron dithiolate hexacarbonyl complexes. This electron density difference was observed by FTIR as aforementioned, in which **1**^{Me} showed bands shifted to lower energy than $Fe_2[(SCH_2)_2NH](CO)_6$.

Dynamic NMR Studies of 1^{Me}

Since **1**^{Me} is asymmetric, all six carbonyl ligands are inequivalent. At 22 °C, the ^{13}C NMR spectrum (in the *C*O region) exhibits only three broad peaks at δ216, 212, and 209. These *C*O sites are located on what is referred to as the rigid iron center (Fe^R) because turnstile rotation of the CO sites is slow on the NMR timescale (Figure 4). At lower temperatures (< -36 °C), the remaining three signals for the CO ligands, those on the non-rigid iron center (Fe^{NR}), appear at δ216, 210, 205. At 41 °C four peaks are observed, three for the CO sites on the Fe^R center, and a broad singlet corresponding to the three CO sites on the Fe^{NR} center that have coalesced. Above 50 °C, only the coalesced signal for the CO sites on the Fe^{NR} center is observed. The differentiation of the $Fe^{NR}(CO)_3$ vs the $Fe^R(CO)_3$ centers is discussed below for the PMe_3-substituted derivative of **1**^{Me}.

The temperature dependence of the rates of two CO interchange processes followed Arrhenius behavior. This analysis revealed that the dynamics at Fe^{NR}proceed with an activation energy barrier of 10.8 (±0.65) kcal/mol, whereas the dynamic process for the Fe^R center occurs with a barrier of 16 (±0.85) kcal/mol. A change in the slope of the Arrhenius plot for the dynamic behavior of the Fe^{NR} center is observed at the extremes of the temperatures used. This suggests that different dynamic process may be in effect at differing temperature ranges, and that the calculated value is an average energy barrier for these processes. It is worth noting that at low temperatures (approaching - 60 °C) the viscosity of the solution could influence the broadness of the peaks in the ^{13}C NMR, and influence the calculations of the energy barriers.

Monosubstituted Derivatives of 1^{Me}

Treatment of **1**^{Me} with phosphine ligands in the presence of $Me_3NO{\cdot}2H_2O$ afforded monosubstituted derivatives $Fe_2(SCH_2N(Me)CH_2)(CO)_5(PR_3)$ (**3**^{Me}, $PR_3 = PMe_3$;**4**^{Me}, $PR_3 = PPh_3$). The ^{1}H NMR signals for the aminothiolate ligand are relatively unchanged in both cases from that of **1**^{Me}. No ^{31}P coupling to the ^{1}H NMR nor the ^{13}C NMR signals is observed. The molecular structure of the PPh_3 derivative **3**^{Me} is similar to that of **1**^{Me} (Figure 5, Table 2). The phosphine is bound to the apical position of the Fe $^{CH2}{}_2$ site (Figure 5). Owing to its low solubility, **3**^{Me} was not examined by DNMR spectroscopy. The overall structure of the PMe_3 derivative **4**^{Me} is again similar to that of **1**^{Me}. The phosphine is however bound to a basal position of the Fe $^{N}{}_1$ site (Figure 5).

The high solubility of **4**^{Me} allowed examination of its low temperature NMR properties. Analogous to **1**^{Me}, three signals, albeit broadened, are observed in its ^{13}C NMR spectrum at

215.8, 210, and 208.8δ at 20 °C (Figure 6). This observation suggests that the Fe^{R} center in **1^{Me}** and **4^{Me}** is $Fe^{CH2}(CO)_3$. Upon cooling to - 60 °C all five CO sites of **4^{Me}** can be resolved, with two new signals corresponding to the Fe^{NR} or $Fe^{NMe}(CO)_2PMe_3$ center present at 216.6 and 208.7δ (see SI). The molecular structure of **4^{Me}** shows that the phosphine occupies the basal site of the Fe^{NR} center octahedral on the side of the sulfur atom. Based on the ^{13}C NMR signals of **4^{Me}** it can concluded that the *C*O site of 1^{Me} that is substituted to form 4^{Me} corresponded to the peak at 205δ in the ^{13}C NMR of 1^{Me}. Coupling to phosphorus is observed for a non-rigid CO site, J_{PC} = 27 Hz, which cannot be specifically assigned based on this data alone. As in **1^{Me}**, the CO sites on the Fe^{R} center begin to coalesce above 20 °C, and are too broad to be observed by NMR spectroscopy.

Disubstituted Derivatives of 1^{Me}

Treatment of **1^{Me}** with dppe (dppe = 1,2-bis(diphenylphosphino)ethane) in the presence of $Me_3NO{\cdot}2H_2O$ afforded the disubstituted derivative $Fe_2[SCH_2N(Me)CH_2](CO)_4$(dppe) (**$5^{Me}$**, Figure 5 and 7). The $^{31}P\{^1H\}$ NMR spectrum shows two signals with J_{PP} of 11.8 Hz. Its ^{13}C NMR spectrum shows four signals in the *C*O region (δ225, 224, 221, 214), each coupled to one phosphorus with J_{PC} of ~ 17 Hz. Due to its poor solubility, **5^{Me}** was not examined by low temperature NMR spectroscopy. The molecular structure of **5^{Me}** confirms its similarity to **1^{Me}**. As with the PMe_3 derivative **4^{Me}**, the phosphine on the Fe $^{N}_{1}$ side is trans to the amine, which causes an elongation of the Fe-N bond. The bridging of two metal centers by a dppe ligand in a similar fashion to that of **5^{Me}** has been observed for related diiron complexes.[11]

Conclusions

$S_2N^{R}_2$ represent a fundamental class of S-N heterocycles, which have eluded study by the organometallic community. We show that they are readily cleaved by Fe(0) reagents to give diiron hexacarbonyls. The new azathiolate complexes are a rare examples of a chiral diiron hexacarbonyl in which the six diastereotopic carbonyl-carbon centers have been identified by NMR. Our ability to conduct these measurements is a result of the high solubility of **1^{Me}** in both polar and non-polar solvents even at very low temperatures (-60 °C).

Compounds containing the S-CH_2-X group appear to be particularly reactive toward iron(0) carbonyls. In related work, the 1,3,5-trithiane is degraded by iron(0) carbonyls to give $Fe_2(SCH_2SCH_2SCH_2)(CO)_6$ as well as the methanedithiolate $Fe_2(SCH_2S)(CO)_6$ (Scheme 1).[12]

The selenium analogues of these complexes have recently been obtained from 1,3,5-triselenocyclohexane.[14]

The pathway leading to **1^{R}** (R = Me, Bn), as well as the SCH_2SCH_2 and $SeCH_2SeCH_2$ compounds is uncertain. With thioethers, iron carbonyls form complexes of the type $Fe(CO)_4(SR_2)$[15] and $Fe_3(CO)_8$ (μ-$SC_4H_8)_2$. [16]

In related work, Hwang and coworkers described the compound $Fe_2[HS(CH_2)_2NCHR](CO)_6$ (R = 2-C_5H_3N-5-Me).[17] The structure of this complex was assigned on the basis of

X-ray crystallography. Thiol ligands bridging two metals have been observed spectroscopically, but are typically very labile.[18] The results described in the present paper suggest that Huang's thiol complex might be reformulated as the $Fe_2[S(CH_2)_2N(H)CHR](CO)_6$ (Figure 8).

Experimental Section

General Considerations

Unless otherwise stated, reactions were conducted using standard Schlenk techniques, and all reagents were purchased from Sigma-Aldrich or Fisher. The heterocycles $S_2N^{Bn}{}_2$, S_2N^{Me}, and $S_2N^{Me}{}_2$ proceeded as reported in the literature.[5, 19] Chromatography was conducted in air on 10 × 2.5 inch columns of silica gel (Silicycle, 40– 63μm). All other solvents were HPLC grade and purified using alumina filtration system (Glass Contour, Irvine, CA). NMR spectra were recorded on Varian UNITY 500 spectrometers. ^{1}H NMR spectra (500 MHz) and ^{13}C NMR spectra (100, 128 MHz) are referenced to residual solvent referenced to TMS. $^{31}P\{^1H\}$ NMR spectra (202 MHz) are referenced to external 85% H_3PO_4. FTIR spectra were recorded on a Perkin-Elmer 100 FT-IR spectrometer. Elemental analyses were done on Exeter Analytical CE 440, and Perkin Elmer 2440, series II analyzers. X-ray crystallography data was obtained on a Bruker SMART instrument with an Apex II detector, using a Copper radiation source.

N,N′-Dimethyl-1,5-dithia-3,7-diazacyclooctane ($S_2N^{Me}{}_2$)

The following is an optimized modification of the literature method.[5] Aqueous methylamine (40 %, 20 mL, 0.23 mmol) diluted with water (50 mL) was treated with cold formalin (34.6 mL, 0.46 mmol). After being stirred for 5 min at 0 °C, this solution was purged with H_2S gas for 2 h causing precipitation of a white solid. After stirring the solution for an additional hour at 0 °C, the precipitate was collected and washed with cold ethanol (100 mL). The precipitate was purified by recrystallization by dissolving in 300 mL of hot acetone followed by cooling to 0 °C. Yield: 5.33 g (52%). ^{1}H NMR (500 MHz, CD_2Cl_2): δ 2.44 (s, 6H, NCH_3), 4.24 (d, 4H, NCH_2S), 4.52 (d, 4H, NCH_2S). ^{13} C NMR (500 MHz, $CDCl_3$): δ38.2 (NCH$_3$), 65.4 (NCH$_2$S). ^{1}H NMR (500 MHZ, CD_2Cl_2, δ): 4.49 (d, 4H, CH_2); 4.25 (d, 4H, CH_2); 2.40 (s, 6H, NCH_3). Anal. Calcd for $C_6H_{14}N_2S_2$: C, 40.41; H, 7.91; N, 15.71. Found: C, 40.50; H, 7.90; N, 15.35. ESI-MS (*m*/*z*): 179 (MH^+).

General Procedure for Reaction of S,N-Heterocycles with $Fe_3(CO)_{12}$

A slurry of the heterocycle and two mole equivalents of $Fe_3(CO)_{12}$ in THF was stirred for 20 h at room temperature under argon. The resulting dark red mixture was evaporated to dryness in vacuo, the residue was extracted in a minimum amount of hexane (15-30 mL). This extract was chromatographed on silica gel eluting with hexanes. Two closely spaced red bands were separated; the first band contained **2**, and the second band contained **1** (see below). Each compound was recrystallized by dissolving in hexanes at room temperature followed by cooling to 0 °C.

$Fe_2[SCH_2N(Me)CH_2](CO)_6(1^{Me})$

The general procedure was applied to the reaction of $S_2N^{Me}_2$ (0.36 g, 2.0 mmol) and $Fe_3(CO)_{12}$ (2 g, 4.0 mmol) in 40 mL of THF. Yield, **2**: 0.09 g (6%). Yield of **1**Me: 0.62 g (84%). ^{13}C NMR (127.7 MHz, d_8-toluene, 20 °C): δ 52.68 (s, 1C, N*C*H$_3$), 57.42(s, 1C, N*C*H$_2$Fe), 73.05 (s, 1C, N*C*H$_2$S). ^{1} H NMR (500 MHz, CD_2Cl_2): δ 2.17 (s, 3H, NC*H*$_3$), 2.73 (d, 1H, NC*H*$_2$Fe), 3.03 (dd, 1H, NC*H*$_2$Fe), 3.52 (d, 1H, NC*H*$_2$S), 4.63 (dd, 1H, NC*H*$_2$S). IR (hexanes): ν_{CO} = 2068 (s), 2024 (vs), 1995 (vs), 1981 (vs), 1964 (s) cm^{-1}. Anal. Calcd for $C_9H_7Fe_2NO_6S$: C, 29.30; H, 1.91; N, 3.80. Found: C, 29.06; H, 1.83; N, 3.70.

$Fe_2[SCH_2N(Bn)CH_2](CO)_6$ (1^{Bn})

The above general procedure was applied to the reaction of $S_2N_2Bn_2$ (0.22 g, 0.67 mmol) and $Fe_3(CO)_{12}$ (0.67 g, 1.3 mmol) in 20 mL of THF. Yield: 0.23 g (77%). ^{1}H NMR (500 MHz, $CDCl_3$): δ 2.49 (d, 1H, NC*H*$_2$Fe), 3.04 (dd, 1H, NC*H*$_2$S), 3.20 (d, 1H, NC*H*$_2$Fe), 3.31 (d, 1H, NC*H*$_2$), 3.42 (d, 1H, NC*H*$_2$), 4.69 (dd, 1H, NC*H*$_2$S), 7.16-7.41 (m, 5H, C$_6$*H*$_5$). IR (hexane): ν_{CO} = 2067 (s), 2024 (vs), 1994(vs), 1980(vs), 1963 (s) cm^{-1}. Anal. Calcd for $C_{15}H_{11}Fe_2NO_6S$: C, 40.48; H, 2.49; N, 3.15. Found: C, 40.55; H, 2.30; N, 3.14.

$Fe_2(SCH_2S)(CO)_6$(2)

The general procedure was applied to the reaction of S_2NMe (0.14 g, 1.0 mmol) and $Fe_3(CO)_{12}$ (1.0 g, 2.0 mmol) in 40 mL of THF. Yield: 0.12 g (33%). ^{1}H NMR (500 MHz, CD_2Cl_2): δ4.65 (s, 2H, SC*H*$_2$S). IR (hexane): ν_{CO} 2079 (s), 2039 (vs), 2007 (vs), 1999 (vs), 1987 (w) cm^{-1}. ^{1}H NMR and IR spectra matched published data.[12]

$Fe_2[SCH_2N(Me)CH_2](CO)_5(PMe_3)(4^{Me}$

A solution of $\mathbf{1^{Me}}$ (0.30 g, 0.811 mmol) in MeCN (50 mL) was treated with $Me_3NO{\cdot}2H_2O$ (0.09 g, 0.811 mmol) in MeCN (30 mL). The solution was stirred for 10 min. at room temperature until all starting material was consumed as detected by FTIR. The resulting dark red solution was treated with PMe_3 (0.062 g, 0.811 mmol), and stirred for an additional 10 min. The solvent was evaporated in vacuo, and the solid was extracted into 5 mL of hexanes and chromatographed on silica (7 in by 0.5 in) in a glovebox. Hexanes were used remove first band followed by 95:5 hexanes: CH_2Cl_2 to obtain $\mathbf{4^{Me}}$. The solvent was removed to yield a red solid that was recrystallized from hexanes at -40 °C. Yield: 0.171 g (45 %). ^{13}C NMR (127.7 MHz, d_8-toluene, 20 °C) δ 13.50 (d, 1C, P(*C*H$_3$)$_3$, J_{PC} = 28.9 Hz),47.29 (s, 1C, N*C*H$_3$), 52.01,(s, 1C, N*C*H$_2$Fe), 67.77 (s, 1C, N*C*H$_2$S), 207.9-215.13 (3s, 3 C, Fe(*C*O)$_3$). ^{31} P{^{1}H} NMR (202.3 MHz, d_2-CH_2Cl_2): δ70.6 (s). IR (CH_2Cl_2): ν_{CO} = 2034 (w), 2021 (w), 1968 (s), 1939 (m), 1905 (w) cm^{-1}. Anal. Calcd for $C_{11}H_{16}Fe_2NO_5PS$: C, 31.68; H, 3.87; N, 3.36. Found: C, 31.67; H, 3.61; N, 3.39.

Reaction of 1^{Me} with PPh_3, and dppe

The diiron complex $\mathbf{1^{Me}}$ and one mole equivalent of the phosphine were dissolved in MeCN or CH_2Cl_2, and treated dropwise with one mole equivalent of $Me_3NO{\cdot}2H_2O$ in MeCN. The resulting mixture was stirred for 3 h at room temperature, and the solvent was evaporated to dryness in vacuo. The red solid was extracted in a minimum amount of CH_2Cl_2 (~10 mL),

and chromatographed on silica gel with CH_2Cl_2 as the eluent. The dried red or orange powders were recrystallized from CH_2Cl_2 with hexanes.

$Fe_2[SCH_2N(Me)CH_2](CO)_5(PPh_3)$ (3^{Me})

The above general procedure was applied to reaction of **1^{Me}** (0.33 g, 0.75 mmol) and PPh_3 (0.20 g, 0.75 mmol) in MeCN (30 mL) followed by a solution of $Me_3NO{\cdot}2H_2O$ (0.083 g, 0.75 mmol) in MeCN (15 mL). Yield: 0.31 g (61%). ^{13}C NMR (127.7 MHz, CD_2Cl_2, 20 °C): δ 64.68 (s, 1C, N*C*H_2Fe), 72.55 (s, 1C, N*C*H_2S). ^{1} H NMR (500 MHz, CD_2Cl_2): δ 1.75 (d, 1H, NC*H*$_2$Fe), 1.79 (d, 1H, NC*H*$_2$Fe), 3.21 (d, 1H, NC*H*$_2$), 3.27 (dd, 1H, NC*H*$_2$S), 3.33 (d, 1H, NC*H*$_2$), 4.16 (dd, 1H, NC*H*$_2$S), 6.96-7.72 (m, 20H, C_6H_5). ^{31}P{^{1}H} NMR (202.3 MHz, d_2-CH_2Cl_2): δ 70.6 (s). IR (hexane): ν_{CO} = 2042 (vs), 1979 (vs), 1971 (vs), 1957 (s), 1924 (s) cm^{-1}. Anal. Calcd. for $C_{26}H_{22}Fe_2NO_5PS$: C, 51.77; H, 3.68; N, 2.32. Found: C, 52.27; H, 3.70; N, 2.48.

$Fe_2[SCH_2N(Me)CH_2(CO)_4(dppe)$ (5^{Me})

The above general procedure was applied to reaction of **1^{Me}** (1.00 g, 2.7 mmol) and dppe (1.08 g, 2.7 mmol) in CH_2Cl_2 (50 mL); treated with $Me_3NO{\cdot}2H_2O$ (0.30 g, 2.7 mmol) in MeCN (35 mL). Yield: 0.821 g (97%). ^{13}C NMR (100.3 MHz, dCD_2Cl_2): δ20.8 (t, 1C, P*C*H_2*C*H_2P), 27.3 (t, 1C, P*C*H_2*C*H_2P), 559.74 (d, 1C, N*C*H_2Fe), 75.46 (d, 1C, N*C*H_2S), 213.54-224.93 (4d, 4C, Fe(*C*O)$_2$).^{1} H NMR (500 MHz, d_2-CH_2Cl_2): δ2.06 (s, 3H, NC*H*$_3$), 2.56 (dd, 1H, NC*H*$_2$Fe), 3.02 (d, 1H, NC*H*$_2$Fe), 3.68 (dd, 1H, NC*H*$_2$S), 5.01 (d, 1H, NC*H*$_2$S), 0.9-2.10 (m, 10H, PC*H*$_2$C*H*$_2$P), 7.37 7.95 (m, 20H, P(C_5H_6)$_2$). $^{[31]}$P $^{20]}$ NMR (202.3 MHz, d_2-CH_2Cl_2): δ 58.44 (d, PC*H*$_2$C*H*$_2$P, Jpp = 12 Hz), 65.65 (d, PC*H*$_2$C*H*$_2$P). IR (hexane): ν_{CO} = 2042 (vs), 1979 (vs), 1971 (vs), 1957 (s), 1924 (s) cm^{-1}. Anal. Calcd for $C_{33}H_{31}Fe_2NO_4P_2S$: C, 55.72; H, 4.39; N, 1.97. Found: C, 55.91; H, 4.34; N, 2.04.

Supplementary Material

Refer to Web version on PubMed Central for supplementary material.

Acknowledgement

This work was funded by the U.S. NIH (grant GM061153-12). We thank Prof. G. S. Girolami for advice on the NMR spectroscopy, Dr. Jeffery Bertke for collecting crystallographic data, and Dr. Raja Angamuthu for help with initial experiments.

References

1. a Linford L, Raubenheimer HG. Adv. Organomet. Chem. 1991; 32:1–119.b Mathur P. Adv. Organomet. Chem. 1997; 41:243–314.c Nametkin NS, Tyurin VD, Kukina MA. Russ. Chem. Rev. 1986; 55:439–454.d Ogino H, Inomata S, Tobita H. Chem. Rev. 1998; 98:2093–2121. [PubMed: 11848961]
2. Nicolet Y, de Lacey AL, Vernede X, Fernandez VM, Hatchikian EC, Fontecilla-Camps JC. J. Am. Chem. Soc. 2001; 123:1596–1601. [PubMed: 11456758]
3. Berggren G, Adamska A, Lambertz C, Simmons TR, Esselborn J, Atta M, Gambarelli S, Mouesca JM, Reijerse E, Lubitz W, Happe T, Artero V, Fontecave M. Nature. 2013; 499:66–69. [PubMed: 23803769]
4. a Angamuthu R, Carroll ME, Ramesh M, Rauchfuss TB. Eur. J. Inorg. Chem. 2011; 2011:1029–1032. [PubMed: 23125531] b Lawrence JD, Li H, Rauchfuss TB, Bénard M, Rohmer M-M. Angew.

Chem., Int. Ed. 2001; 40:1768–1771.c Li H, Rauchfuss TB. J. Am. Chem. Soc. 2002; 124:726–727. [PubMed: 11817928]

5. Akhmetova VR, Nadyrgulova GR, Niatshina ZT, Dzhemilev UM. Chem. Heterocycl. Compd. 2009; 45:1155–1176.
6. Wilson AD, Fraze K, Twamley B, Miller SM, DuBois DL, Rakowski DuBois M. J. Am. Chem. Soc. 2008; 130:1061–1068. [PubMed: 18163630]
7. Jacobsen, NE. NMR Spectroscoy Explained. Simplified Theory, Applications and Examples for Organic Chemistry and Structural Biology. John Wiley & Sons, Inc.; Hoboken, New Jersey: 2007.
8. Adams RD, Babin JE. Organometallics. 1988; 7:963–969.
9. Long L, Xiao Z, Zampella G, Wei Z, De GL, Liu X. Dalton Trans. 2012; 41:9482–9492. [PubMed: 22751866]
10. Felton GAN, Mebi CA, Petro BJ, Vannucci AK, Evans DH, Glass RS, Lichtenberger DL. J. Organomet. Chem. 2009; 694:2681–2699.
11. a Ezzaher S, Capon J-F, Gloaguen F, Pétillon FY, Schollhammer P, Talarmin J. Inorg. Chem. 2007; 46:9863–9872. [PubMed: 17941631] b Adam FI, Hogarth G, Kabir SE, Richards I. C. R. Chim. 2008; 11:890–905.
12. Raubenheimer HG, Linford L, van A. Lombard A. Organometallics. 1989; 8:2062–2063.
13. Shaver A, Fitzpatrick PJ, Steliou K, Butler IS. J. Am. Chem. Soc. 1979; 101:1313–1315.
14. Harb MK, Niksch T, Windhager J, Görls H, Holze R, Lockett LT, Okumura N, Evans DH, Glass RS, Lichtenberger DL, El-khateeb M, Weigand W. Organometallics. 2009; 28:1039–1048.
15. a Cane DJ, Graham WAG, Vancea L. Can. J. Chem. 1978; 56:1538–1544.b Meng X, Bandyopadhyay AK, Fehlner TP, Grevels F-W. J. Organomet. Chem. 1990; 394:15–27.c Cotton FA, Kolb JR, Stults BR. Inorg. Chim. Acta. 1975; 15:239–244.
16. Cotton FA, Troup JM. J. Am. Chem. Soc. 1974; 96:5070–5073.
17. Wu C-Y, Chen L-H, Hwang W-S, Chen H-S, Hung C-H. J. Organomet. Chem. 2004; 689:2192–2200.
18. a Apfel U-P, Troegel D, Halpin Y, Tschierlei S, Uhlemann U, Görls H, Schmitt M, Popp J, Dunne P, Venkatesan M, Coey M, Rudolph M, Vos JG, Tacke R, Weigand W. Inorg. Chem. 2010; 49:10117–10132. [PubMed: 20873759] b Dong W, Wang M, Liu X, Jin K, Li G, Wang F, Sun L. Chem. Commun. 2006:305–307.c Zaffaroni R, Rauchfuss TB, Gray DL, De Gioia L, Zampella G. J. Am. Chem. Soc. 2012; 134:19260–19269. [PubMed: 23095145]
19. a Cadenas-Pliego G, de Jesus Rosales-Hoz M, Contreras R, Flores-Parra A. Tetrahedron: Asymmetry. 1994; 5:633–640.b Leonard NJ, Conrow K, Yethon AE. J. Org. Chem. 1962; 27:2019–2021.
20. Abel EW, Mittal PK, Orrell KG, Sik V. J. Chem. Soc., Dalton Trans. 1986:961–966.

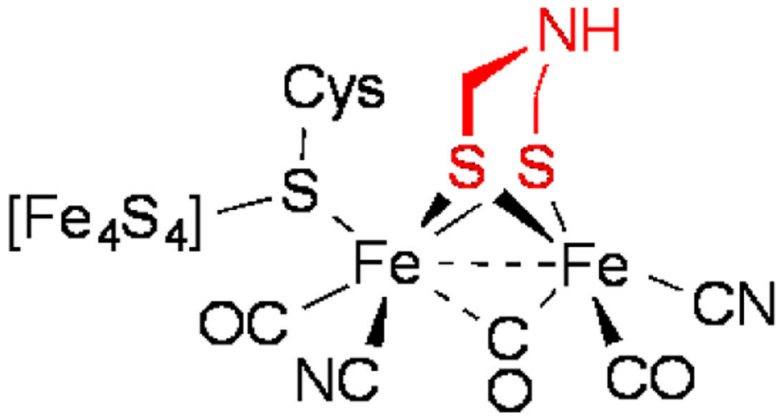

Figure 1.
Active site of [FeFe]-hydrogenase highlighting the azadithiolate cofactor.

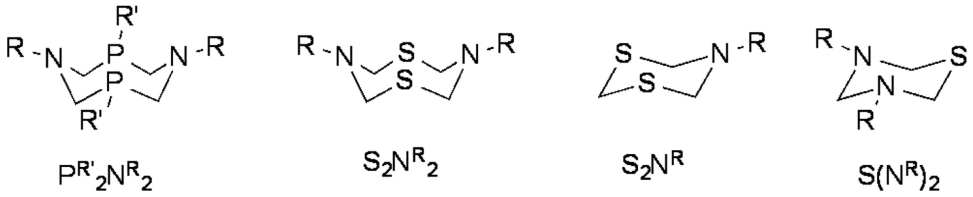

Figure 2.
Heterocyclic compounds discussed in this work.

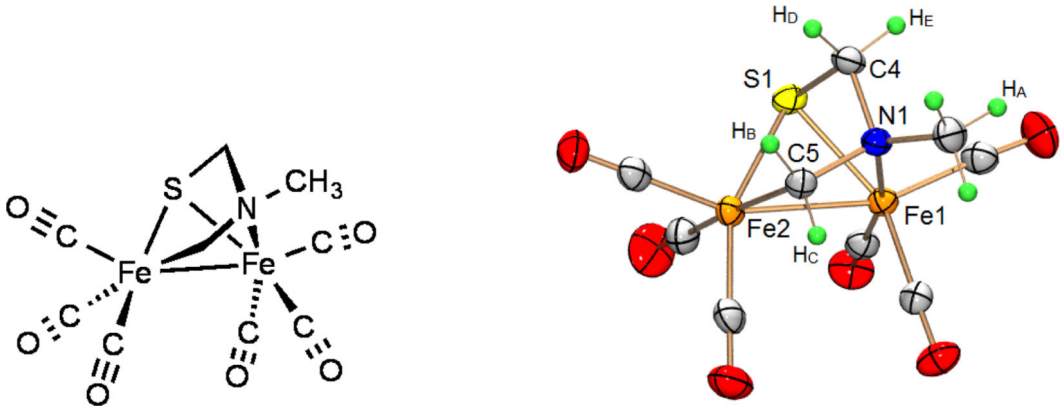

Figure 3.

Two depictions of $Fe_2[SCH_2N(Me)CH_2](CO)_6$ (**1**^{Me}) (thermal ellipsoids at 50% probability level).

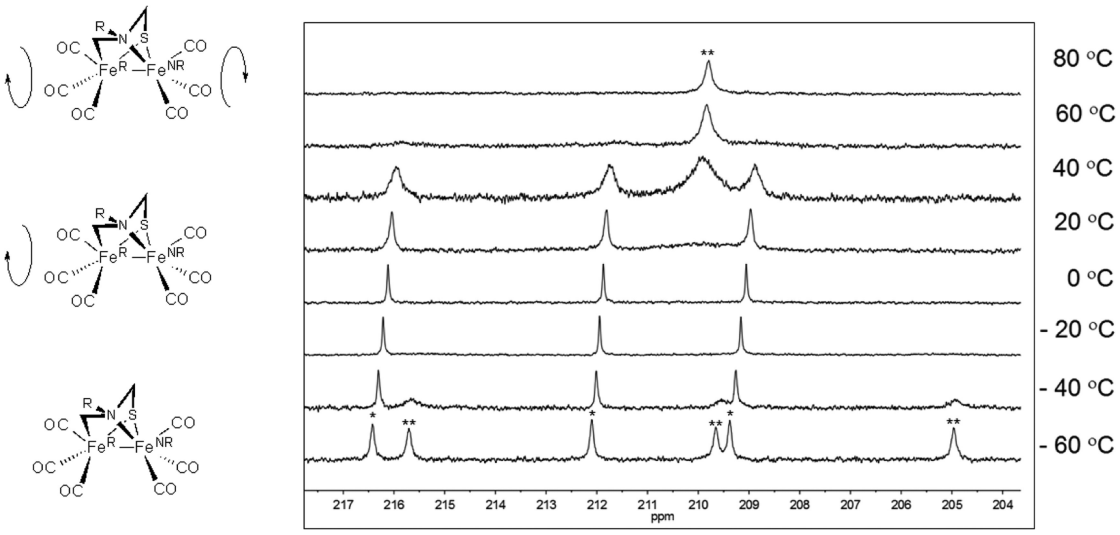

Figure 4.

Representation of dynamic processes of **1**$^{\mathbf{Me}}$; Fe^{NR} = non-rigid, Fe^{R} = rigid. ^{13}C NMR spectra (125.7 MHz, d_8-toluene solution) of compound **1**$^{\mathbf{Me}}$ at various temperatures (right). The average chemical shifts for the CO signals on the Fe^{R} and Fe^{NR} centers are indicated with * and **, respectively.

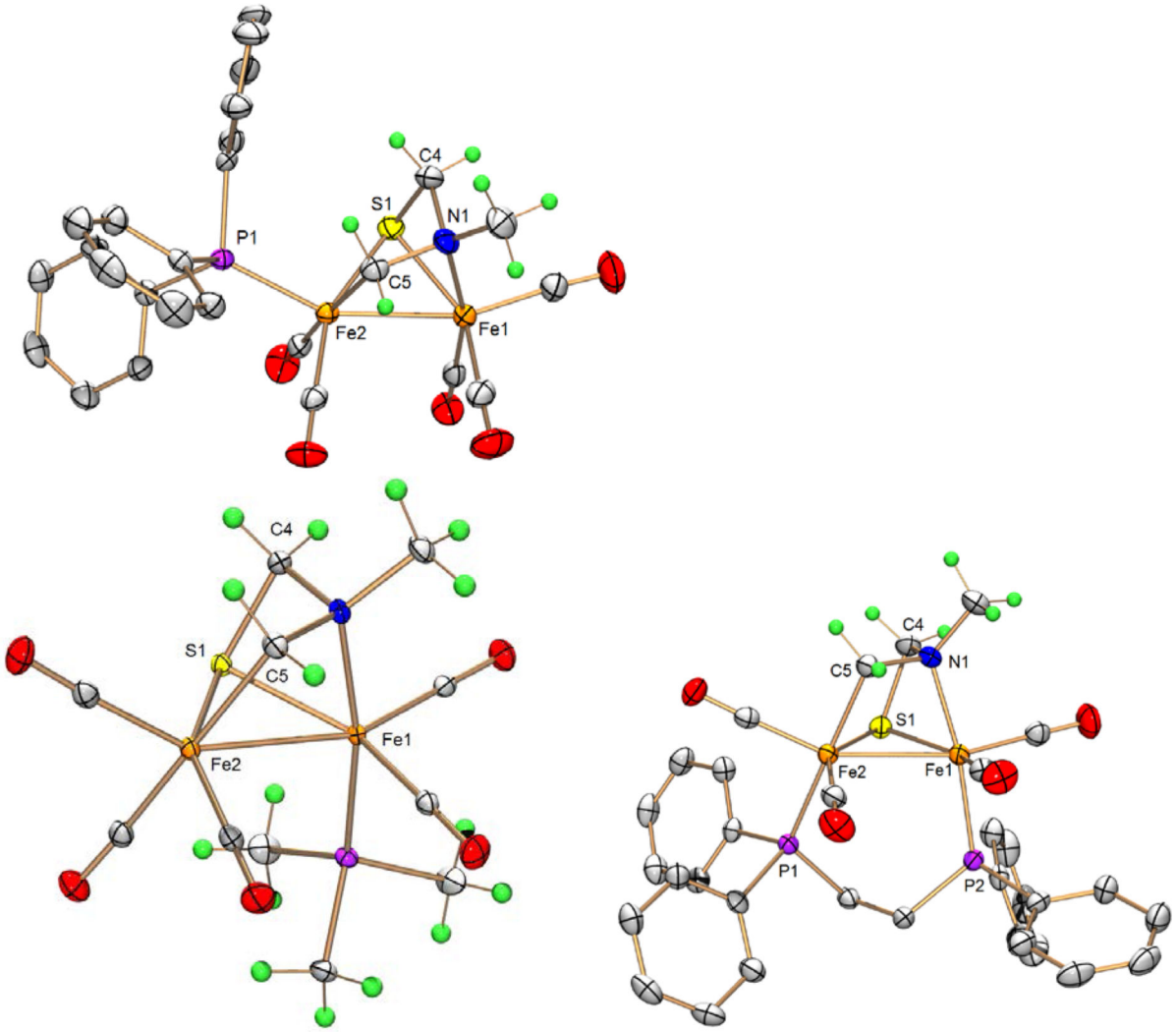

Figure 5.

ORTEP of $Fe_2[SCH_2N(Me)CH_2](CO)_5(PPh_3)$ ($\mathbf{3}_{Me}$, top left), $Fe_2[SCH_2N(Me)CH_2](CO)_5(PMe_3)$ ($\mathbf{4}^{Me}$, top right), and $Fe_2[SCH_2N(Me)CH_2](CO)_4(dppe)$ ($\mathbf{5}^{Me}$, bottom) with 50% probability thermal ellipsoids.

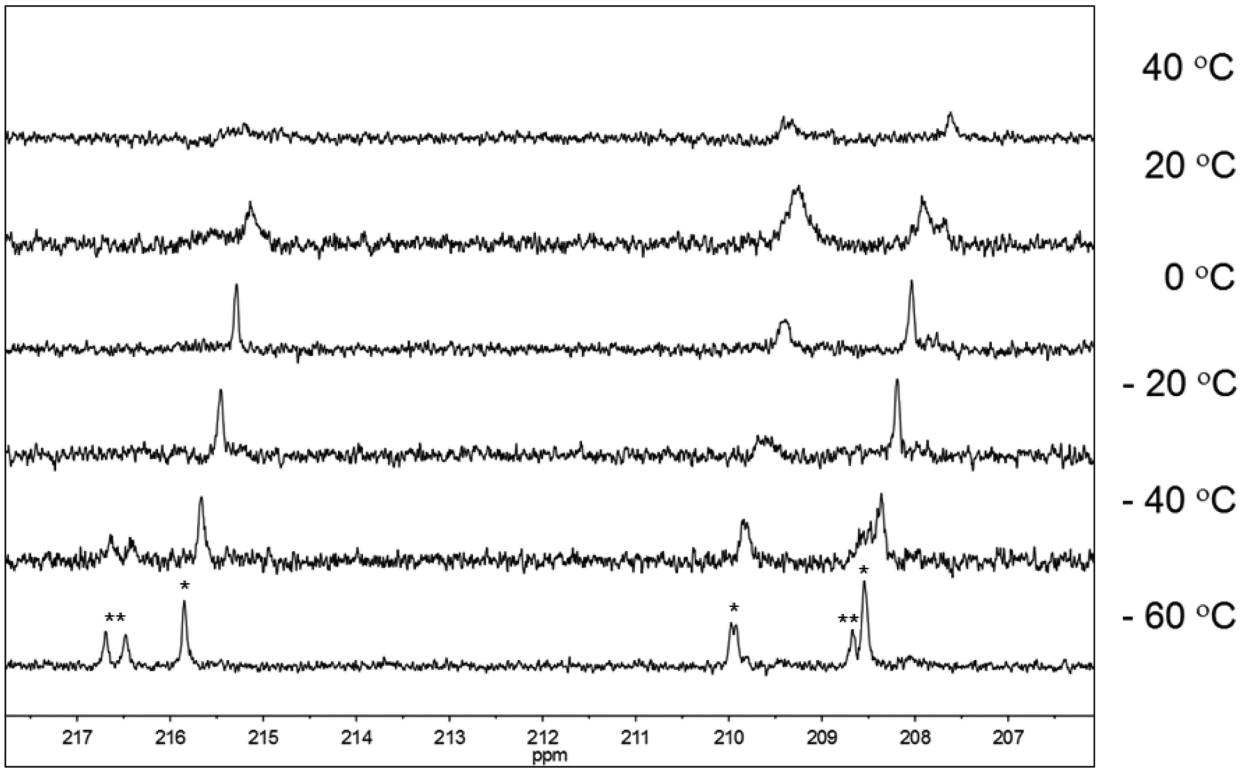

Figure 6.

^{13}C NMR spectra (125.7 MHz, d_8-toluene solution) of **4^{Me}** at various temperatures. Signals assigned to $Fe^{R}(CO)$ (corresponding to $Fe^{CH2}(CO)_3$) and Fe^{NR} (CO) (corresponding to $Fe^{NMe}(CO)_2PMe_3$) are indicated with * and **, respectively.

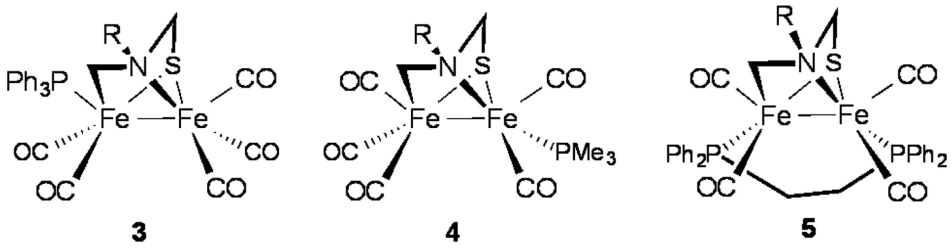

Figure 7.
Structures of the substituted derivatives of $\mathbf{1^{Me}}$.

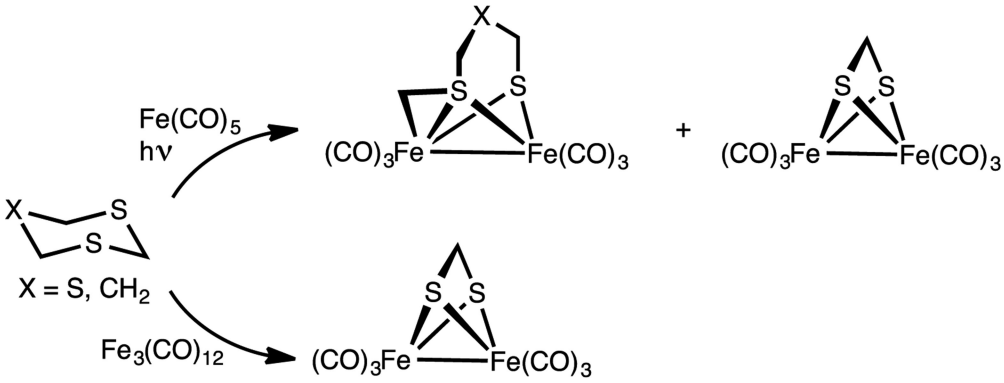

Scheme 1.

Activation of saturated C-S heterocycles by iron carbonyls, which are reminiscent of the results in this report.[12-13]

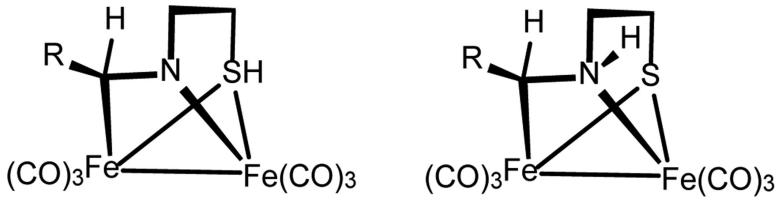

Figure 8.

Structures proposed by Huang et al (left)[17] and by this work for $Fe_2(RCHNC_2H_4S)(CO)_6$ (R = 2-methylpyridyl) (right).

Table 1

Dihedral Angles and H-H Coupling Constants for the -CH2-N-CH2-S- Ligand of 1Me.

Plane 1	Plane 2	Dihedral Angle (°)
H_B-C_5-N	N-C_4-H_D	52.9
H_B-C_5-N	N-C_4-H_E	126
H_C-C_5-N	N-C_4-H_D	130
H_C-C_5-N	N-C_4-H_E	10.7

Nucleus 1 (δ)	Nucleus 2 (δ)	$^{n}J_{HH}$ (Hz)
H_A (2.17)	-	-
H_B (2.73)	H_C (3.02)	7.34 (n = 2)
H_C (3.02)	H_E (4.62)	2.91 (n = 4)
H_D (3.51)	H_E (4.62)	7.54 (n =2)

Table 2

Bond distances of interest for crystallographically characterized complexes. All distances are given in angstroms.

	Fe_1-Fe_2	Fe_1-N_1	Fe_2-C_5	Fe_1-S_1	Fe_2-S_1	Fe_n-P_m
$\mathbf{1^{Me}}$	2.5702 (4)	2.033 (18)	2.055 (2)	2.258 (6)	2.248 (6)	-
$\mathbf{3^{Me}}$	2.5771 (4)	2.035 (16)	2.062 (2)	2.268 (6)	2.250 (6)	Fe_2-P_1: 2.219 (6)
$\mathbf{4^{Me}}$	2.623 (5)	2.039 (2)	2.066 (2)	2.260 (6)	2.249 (6)	Fe_1-P_1: 2.211 (8)
$\mathbf{5^{Me}}$	2.648 (4)	2.047 (18)	2.018 (18)	2.280 (6)	2.250 (5)	Fe_1-P_1: 2.217 (7)
						Fe_2-P_2: 2.222 (6)